Chem. Senses 31: 359–369, 2006

doi:10.1093/chemse/bjj040
Advance Access publication March 1, 2006

Temporal Integrity of an Airborne Odor Stimulus is Greatly Affected by Physical Aspects of the Odor Delivery System

Richard S. Vetter[1], Amy E. Sage[1], Kristine A. Justus[1], Ring T. Cardé[1] and C. Giovanni Galizia[1,2]

[1]Department of Entomology, University of California, Riverside, CA 92521, USA and
[2]Universität Konstanz, D-78457 Konstanz, Germany

Correspondence to be sent to: C. Giovanni Galizia, Universität Konstanz, D-78457 Konstanz, Germany. e-mail: giovanni.galizia@uni-konstanz.de

Abstract

There is currently a debate about the role played by temporal patterns in neural activity in olfactory coding. An accurate analysis of this question, however, is only possible if the temporal properties of a stimulus itself are well defined. So far, no technique with sufficient temporal resolution has been available to accomplish this. Using a photoionization detector (PID), we show that the configuration of the odor delivery apparatus and the airflow settings greatly influence the integrity of a stimulus profile within an odor delivery apparatus. In a situation where pulsatile odor stimuli are applied to a stationary preparation, we tested the effect of 1) axial and off-center location within the airstream, 2) airflow of the odor delivery, 3) exit tube length, 4) exit tube diameter, 5) orientation of the odor delivery device in relation to the exhaust flow, and 6) exhaust tube air speed. This has important implications for the study of time in olfaction; significant planning must be incorporated into the design of the experiment to provide a well-defined odor delivery system.

Key words: odor delivery, olfactometer, photoionization detector, temporal patterns, turbulence

Introduction

Airborne odors consist of volatile substances that are transported in air. In a natural environment, moving air is turbulent, so that odor sources create complex spatiotemporal sequences of high and low concentrations interspersed with gaps of odor-free air (Murlis *et al.*, 1992). In most physiological experiments, a reductionist approach avoids such complexities by using on–off (square) odor pulses or trains of odor pulses. Thus, the parameters being investigated are reduced to odor identity and stimulus concentration. The term ''olfactometer'' is often used for an odor delivery system and is used with that meaning here. Differences in design and properties of olfactometers are many: some are best for delivering a large quantity of different chemicals, and others are better suited for accurately controlling odor concentration or timing (Kauer and Firestein, 1995; Galizia *et al.*, 1997; Slotnick and Schellinck, 2001; Johnson *et al.*, 2003). For example, the first olfactometer was developed by Zwaardemaker in 1888 and controlled odor concentration by covering different portions of an odorous glass rod with a rubber tube, whereas odor identity was manipulated by exchanging both the glass rod and the rubber tube (Zwaardemaker, 1889; Finger, 1994).

It is generally difficult to determine how an airborne odor, once released from its source, travels to the animal's sensory organ. In olfactometer design, surrogate substances such as CO_2 or ''smoke'' are often used for calibration in air (Kauer and Firestein, 1995; Mafra-Neto and Cardé, 1995), whereas aquatic systems allow mixing fluorescent tracers (Weissburg and Dusenbery, 2002). Olfactory stimuli can be well controlled in wind tunnels, where the entire airflow is laminar, and both the odor release site and experimental animals are small with respect to the moving air. Wind tunnels have been applied successfully to behavioral studies of pheromone detection in moths (Willis and Baker, 1984; Mafra-Neto and Cardé, 1995). However, this approach is more problematic in physiological experiments designed for olfactory stimulation of a stationary preparation, where the experimental apparatus is large relative to the area of measurement and the apparatus itself creates a turbulent flow. At the other extreme of experimental parameter control, turbulence is purposely created, and its occurrence becomes part of the experimental design (Bau *et al.*, 2002; Justus *et al.*, 2002b, 2005; Stopfer and Laurent, 2002). The temporal occurrence of odor plumes strongly affects responses of olfactory

receptor neurons (Rumbo and Kaissling, 1989; Barrozo and Kaissling, 2002; Bau *et al.*, 2002), central pathways (Christensen *et al.*, 1996; Heinbockel *et al.*, 1999; Vickers *et al.*, 2001), and the behavioral responses in insects (Baker *et al.*, 1988; Christensen *et al.*, 1996).

In many experiments, information about whether and to what degree turbulence affects stimulus integrity is unknown. The difficulty arises from the lack of high-speed, high-sensitivity physical measurement devices that can measure temporal properties of an olfactory stimulus. Recently, photoionization detectors (PIDs) with high temporal resolution have been developed. PIDs are often used to monitor gases (e.g., gas leaks), but they also allow measurement of airborne substances that are general odorants, such as hexanol, heptanone, and many more. A PID cannot identify an odor unless it is coupled to a chromatographic column, but it can quantify cumulative concentration of all detectable gases. Such a detector has been used to improve our understanding of the structure of insect pheromone plumes as they move downwind (Justus *et al.*, 2002a) and to determine response properties of insect antennae in chaotic pheromone plumes (Justus *et al.*, 2005). A slower PID has already been integrated into an olfactometer for concentration control (Johnson *et al.*, 2003). However, how the temporal structure of a stimulus is influenced by an experimental setup has not yet been investigated. Using the PID, we found that the temporal structure of pulsatile odor stimuli disintegrated within 10–20 mm from the tubing exit at the airflow we employed (5–10 ml/s). It was equally surprising how small changes in the physical variables of the setup significantly improved or degraded the characteristics of the pulsatile odor stimulus. We present this information here in regard to maximizing signal coherence in future experiments, such that results from measurements in the olfactory system will be more readily interpretable.

Materials and methods

Basic setup

The basic setup involved a mini-PID fast-response PID with frequency response of 330 Hz, sensitivity of 50 ppb (for propylene; propylene was not used in this study; the sensitivity to 2-heptanone is unknown), an air sampling rate of 1.5 L/min, and a cross-sectional sampling area of approximately 0.58 mm^2 (Model 200a, Aurora Scientific Inc., Canada). The analog PID output (0–10 V) was hooked up to an Intelligent Data Acquisition Collector, IDAC-4-USB (Syntech, The Netherlands). No attempt was made to calibrate PID output voltage with absolute odor concentration. Because the gain of the PID can be continuously adjusted, absolute values differed for measurements on different days, that is, the "PID response" axis in the figures has arbitrary units. Data were analyzed with Autospike 32 program (Syntech) and with custom-written programs in Interactive Data Language (Research Systems, Inc, Boulder, CO). Airflows were delivered via a Stimulus Flow Controller, SFC-2 (Syntech), henceforth referred to as the puffer. Airflow was supplied from an air tank channeled through the puffer, such that a mainstream airflow was delivered through Tygon tubing [5-mm internal diameter (ID)] through a stimulus tube consisting of a plastic pipette tip (Fisher Brand, #02-681-172, 200–1300 µl, 7-mm ID large opening with a 78-mm length before cutting), which was cut on the tapered end such that it was 61-mm long with a 4.5-mm ID opening on the smaller end (Figure 1). At 31 and 25 mm from the large end of the stimulus tube tip, 1.6-mm diameter holes were drilled into the side to allow entrance of borosilicate glass Pasteur pipettes (143-mm length) that delivered the stimulus airflows. The hole at 25 mm accommodated the odorant pipette, and the hole at 31 mm accommodated the complementary air pipette. This latter glass pipette delivered the same rate of clean air during non-odor periods, as did the odorant pipette of odorized air during stimulation, and therefore the final airflow at the exit remained constant throughout. These two Pasteur pipettes were connected to the puffer with 5-mm Tygon tubing and plastic pipette tips cut to 61-mm length. A third hole (1.6-mm diameter) was drilled 12 mm from the opening end of the stimulus tube tip for insertion of the PID. When the PID was not inserted into the stimulus tube, a piece of tape covered the hole. The direction of the exit flow of the odor from the stimulus tube was parallel and in the same direction as a constant background airflow provided by a hood (0.4 m/s). Airflows from the puffer were controlled directly by the puffer; air speed of the exhaust was measured with an anemometer (Lutron LM-8000, Lutron Electronic, Taiwan).

A PID can detect a variety of chemicals which can be ionized by a strong light source. We used 2-heptanone in all experiments as the odor detected by the PID. To prepare the odor, four filter paper circles (Whatman no. 1, 1-cm diameter) were placed into the large end of the glass Pasteur pipette, against the walls, and 5 µl of 2-heptanone was pipetted onto each piece of filter paper. The odor-loaded pipette was immediately placed in-line with the puffer apparatus and

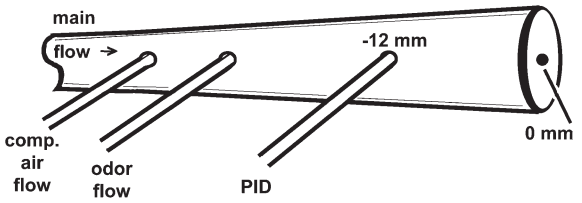

Figure 1 Basic setup of the odor delivery apparatus. Holes were drilled into the side of a plastic pipette tip. Mainstream airflow was delivered through the narrow end of the tip. Clean air and odor-laden air were each delivered through a glass Pasteur pipette at the respective ports to ensure equal final airflows. When odor was delivered, the complementary airflow was shut off using an automated stimulus flow controller and flow was switched to the odor flow. The PID is shown at the −12-mm port to indicate but one of the tested positions (compare with Figure 3).

left for 30 min to equilibrate before testing. Then, a few preliminary puffs were run to ensure that the PID response was not off scale in the Autospike program.

Stimulus delivery

Samples of 2-heptanone were delivered over the PID at 1) a single pulse of 3-s duration and 2) a series of 10 pulses of 50-ms duration at 3.3 Hz. The 3-s pulse allowed determination of the deviation from a flat square wave, and the 10 pulses allowed determination of the coherence at the detector to the odor emission signal. For most settings, odor/mainstream airflows were delivered at four rates (0.5 ml/s odor pipette into 4.5 ml/s mainstream air, referred to as 0.5/4.5, and similarly 1/4, 1/9, and 2/8).

Baseline degradation of odor delivery

Repeatedly releasing odor-laden air from a Pasteur pipette leads to a reduction of odor concentration over time. Initial experiments were performed to determine this odor concentration decrease in order to correct for it mathematically. The PID was inserted into the stimulus tube at the hole 12 mm from the exit such that the PID tube was in the center of the airstream. A 3-s pulse was delivered every min for 2 h and recorded. Odor-laden air was delivered at 0.5 ml/s, and mainstream air was delivered at 4.5 ml/s. During this 2-h period, the response dropped approximately 75% from the initial pulses (Figure 2A). This baseline experiment was performed three times with almost identical results and an average fit-to-curve single exponential equation ($y = 1 \times e^{-0.014x}$) was calculated (Figure 2B; the equation in the Figure is for a single fit).

During subsequent experiments, we adhered to this one-application-per-min period throughout, both for the continuous 3-s pulse and for the series of 10 short pulses. Therefore, the degree of degradation should be similar to that found above, although not identical, because the degradation caused by a pulsed stimulus is likely to be different from that of a continuous 3-s pulse. We then adjusted the measured responses by applying the decay curve correction to obtain reliable response magnitudes over time. Except for a few times when the apparatus needed to be rearranged, we were able to maintain this once-per-min schedule of odor delivery; however, mostly 2 min and no more than 4 min expired between pulses during changes of the physical configuration of the setup. We ran most assays for no more than an hour with a few extending to 70 min.

Data analysis

In order to quantify the integrity of a delivered stimulus at a certain position, we chose two observable variables using a continuous pulse and a train of short pulses. First, with a continuous 3-s odor pulse, we estimated the odor concentration at a certain position by calculating the mean PID response at that position, and we measured how smooth

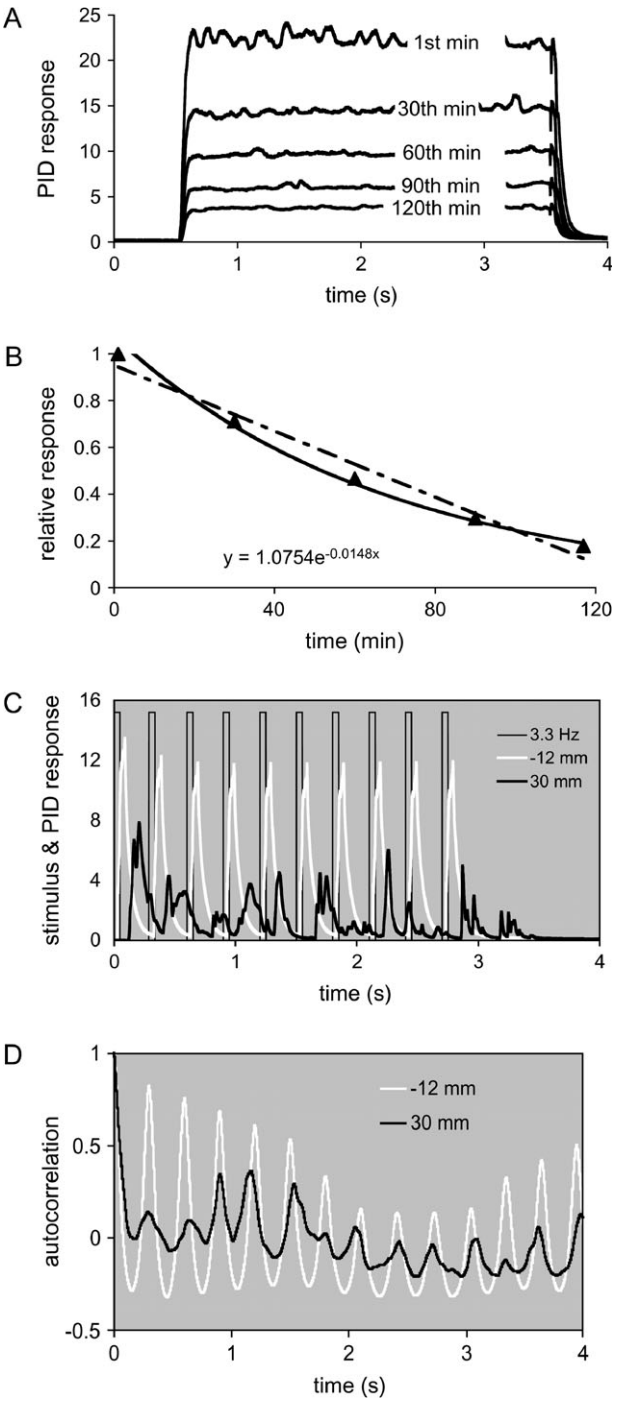

Figure 2 Explanation of the data determination and analysis. **(A)** Responses of the PID (arbitrary units) to continuous 3-s pulses of 2-heptanone over a 2-h period degrade with time. **(B)** Fit-to-curve equation for the 2-h degradation. The interrupted line is a linear fit; the continuous line an exponential fit. **(C)** Response of the PID to 10 pulses delivered at 3.3 Hz. The thin black line shows the ideal odor emission pattern produced by the puffer (digital control current). PID responses are shown with the PID at −12 mm (white line) and at 30 mm (thick black line). **(D)** Autocorrelation analysis of data from Figure 2C. There is high coherence for the −12-mm data (white line—uniform occurrence of peaks, high peak-to-trough distances, smooth curves) and lower coherence for the 30-mm data (black line—peaks less uniform, lower peak-to-trough distance, jagged curve).

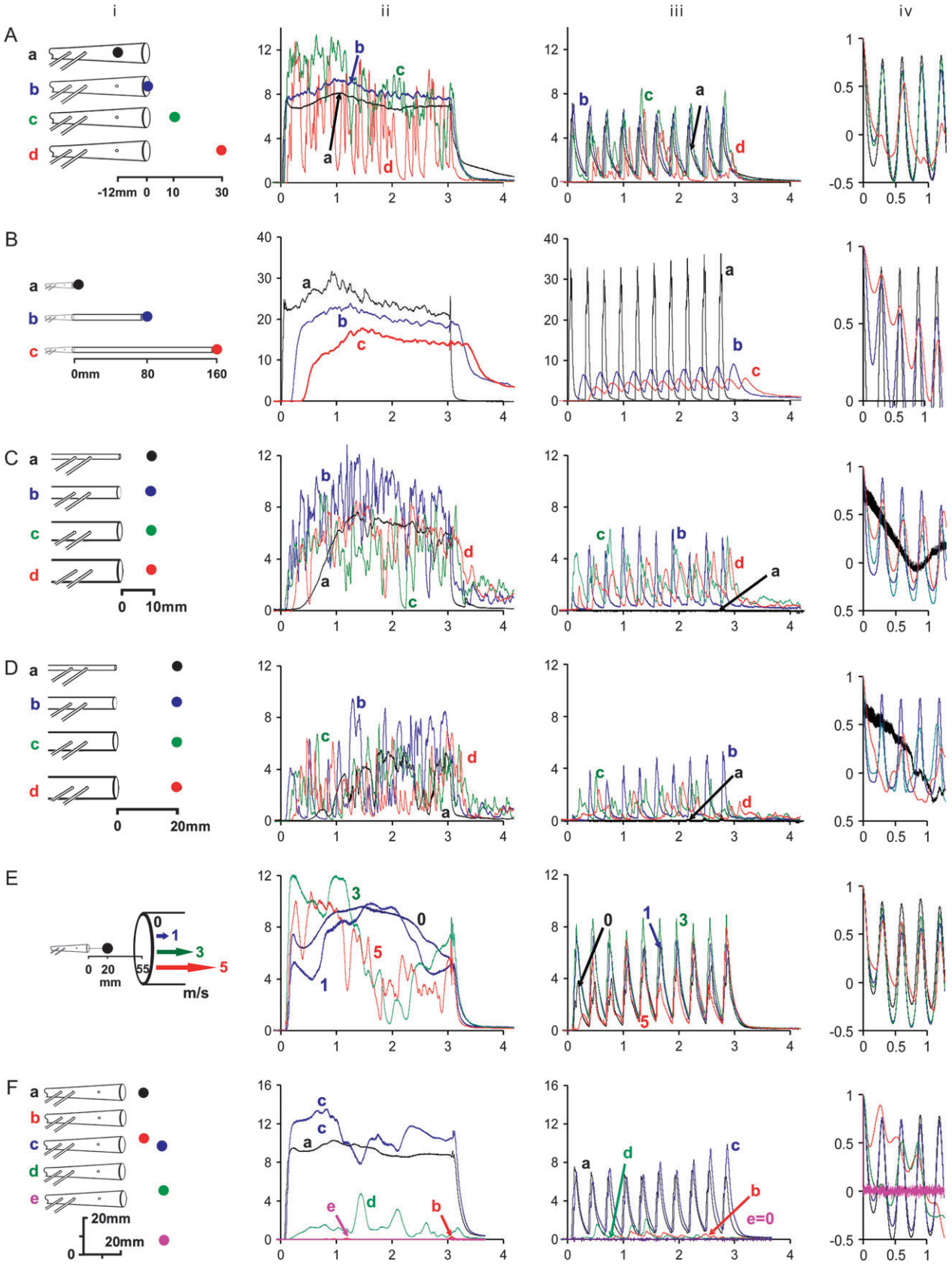

the response was, by calculating the standard deviation (SD) of the response over the 3-s odor delivery.

For the second statistic, we quantified how well a temporal pattern in the stimulus was maintained at the varied positions of the PID. We delivered a train of 10 single pulses of 50-ms duration each at 3.3 pulses/s and calculated an autocorrelation on the measured PID responses. Autocorrelation is calculated by computing the correlation coefficient between a response trace and itself, shifted by an increasing time lag; therefore, at time lag 0 the autocorrelation is always 1. With a periodic structure in the signal, the autocorrelation returns to high values periodically. Because we gave 10 test pulses, peak values decrease over time because the number of periodic events that overlap decrease with increasing time lag. A sinusoidal autocorrelation indicates that the repetition pattern in the stimulus is maintained, while a loss in temporal pulse structure will result in a flat or chaotic autocorrelation trace (Figure 2C,D).

The experiment "position along airstream" was replicated five times. Because the measured variation was low, additional experiments were generally only performed once. For clarity, all figures show the mean for one continuous 3-s pulse at specific odor/mainstream airflows and at the physical parameters being tested with SD as error bar (bar charts in Figures 4–8). The 3.3-Hz data for the same parameters are presented as an autocorrelation analysis, shifted along the *y*-axis for clarity such that the absolute values have no significance (line graphs in Figures 4–8).

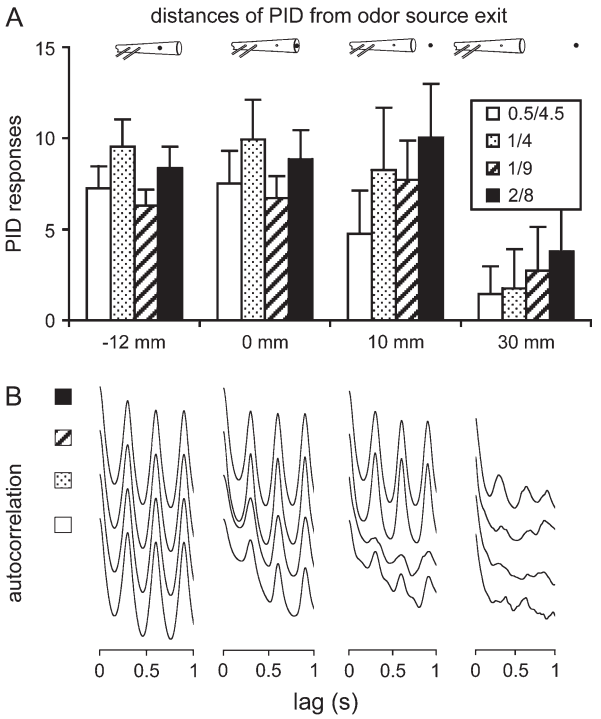

Figure 4 Effect of distance along airstream (see also Figure 3A). **(A)** PID responses at differing odor/mainstream airflows and distance from odor source exit for continuous 3-s pulses. Higher airflow values indicate better pulse integrity (more detected molecules). Error bars are SD of response, with small bars indicating a smooth response. **(B)** Autocorrelation analysis for the 3.3-Hz pulses; each graph is aligned below the distance (in Figure 4A) to which it is complementary. A sinusoidal trace indicates that the temporal pulsed patterns in the stimulus are maintained.

Position along airstream

To determine the integrity of the pulse with distance, we positioned the PID within the stimulus tube (−12 mm), at the exit of the stimulus tube (0 mm), at 10 mm, and at 30 mm from the exit with the tip of the PID in the center of the flow (Figures 3A and 4). Airflows were 0.5/4.5, 1/4, 1/9, 2/8 (ml/s odor/ml/s continuous), which at stimulus tube exit corresponds to air speeds of 0.13 m/s (for 0.5/4.5 and 1/4) and 0.26 m/s (for 1/9 and 2/8). Exhaust speed was 0.4 m/s.

Effect of exit tube length

The setup above was tested similarly with an extension of 8- and 16-cm Tygon tubing (8-mm ID) placed on the end of the stimulus tube to determine the effects of tube length on the stimulus (Figures 3B and 5). In all cases, the PID was placed at the exit of the stimulus tube. Tests were run at airflows 0.5/4.5, 1/4, 1/9, 2/8 and for the 16-cm length also at airflows 4/6, 4/12, 4/16 (ml/s odor/ml/s continuous). High airflows were tested to determine if this reestablished pulse integrity. Exhaust speed was 0.4 m/s.

Effect of exit tube diameter

The system above was tested with a 45-mm long piece of tubing of four diameters (1.3, 4.8, 8.1, and 9.2 mm). These tubes

Figure 3 Characteristic responses for the PID with the varying parameters. The position of the PID in each experimental configuration is designated by the solid colored dot. All abscissae are in seconds. Unit labeling on abscissae and ordinates have been omitted to save space. Columns: column i shows the configuration of the setup; parameters are shown graphically. A colored letter designating the variable matches the color of the corresponding dot (PID position) and the color of the data line in the graphs in columns ii–iv. All data shown here were recorded with the odor flow at 2 ml/s and the mainstream flow at 8 ml/s. Column ii shows individual assay responses to a 3-s continuous pulse, ordinate is PID response (arbitrary units, labeling omitted to save space). Column iii shows individual assay responses to 10 pulses delivered at 3.3 Hz, ordinate is PID response (same arbitrary units as in ii). Column iv shows autocorrelation analysis of the data in column iii, ordinate is autocorrelation value. Rows: rows A–F show the different setups, which are treated in detail in subsequent figures. Row A: effect of distance along airstream (best setting: within tube, see Figure 4). Row B: effect of tube length (best setting: short, see Figure 5). Rows C and D: effect of tube diameter with the PID at 10 mm and at 20 mm from exit of the stimulus tube (best setting: intermediate, see Figure 6). Row E: effect of varying exhaust air speed (best setting: intermediate, see Figure 7). Row F: effect of PID placement off of centerline (best setting: right on the axis, see Figure 8). Because some overlaid traces are difficult to follow individually, each row is given as a separate figure with isolated traces in the supplementary material on the Web (Figures S3A–S3F, see http://neuro.uni-konstanz.de/PID or supplementary material on the Journals website).

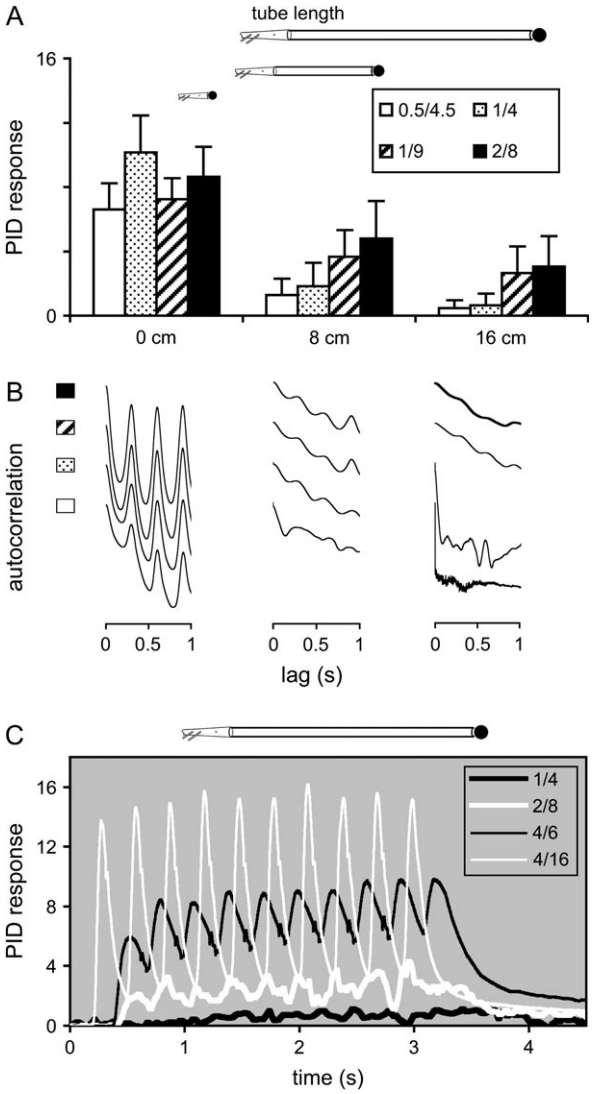

Figure 5 Effect of tube length (see also Figure 3B). **(A)** PID response at differing tube lengths for continuous 3-s pulses. A higher value indicates a better condition. Error bars are SD of response, with small errors indicating a smooth response. **(B)** Autocorrelation analysis for the 3.3-Hz pulses; each graph is aligned with Figure 5A. Pulses are already lost at 8-cm tube length. **(C)** PID response to 3.3-Hz pulses delivered at four airflows. The PID was placed at the end of the 16-cm tubing. Faster air speeds can partially rescue the temporal odor pattern.

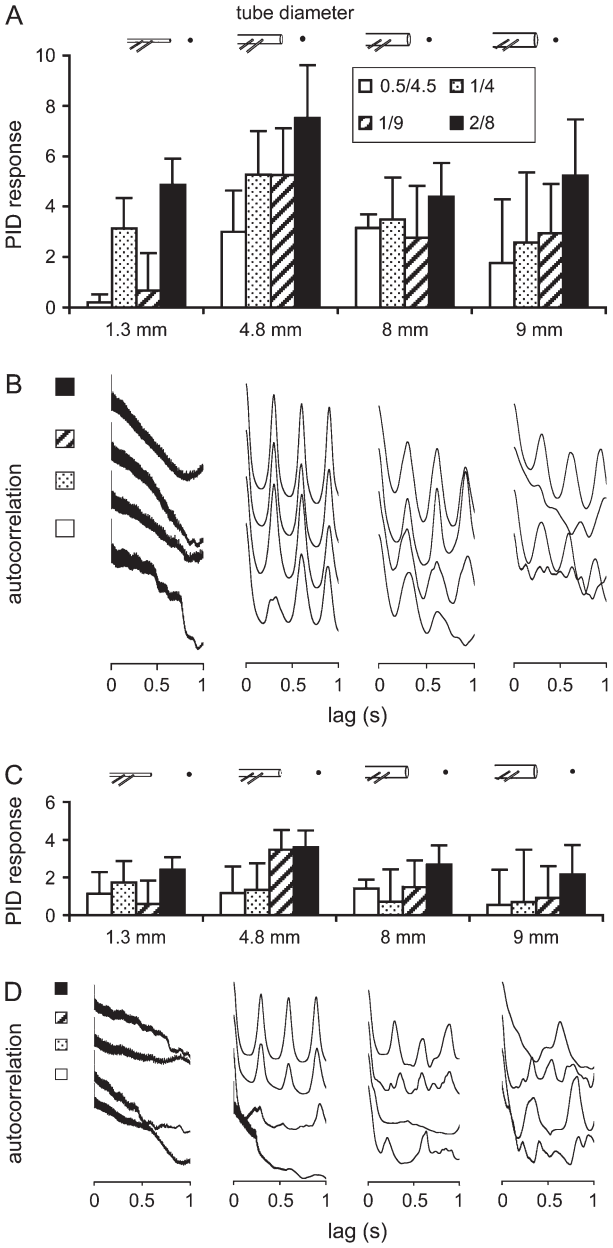

Figure 6 Effect of tube diameter (see also Figure 3CD). **(A)** PID response at differing tube diameters for continuous 3-s pulses with the PID at 10 mm downstream from the tube exit. **(B)** Corresponding autocorrelation analyses for the 3.3-Hz pulses. **(C)** PID response at differing tube diameters for continuous 3-s pulses with the PID at 20 mm downstream from the tube exit. **(D)** Autocorrelation analysis for the 3.3-Hz pulses. Best tracking is achieved with the 4.8-mm diameter tube.

were inserted at the end of or over the end of the 5-mm ID Tygon tubing delivering the air from the puffer. The PID was positioned in the center of the flow at 10 mm (Figures 3C and 6A,B) and 20 mm from the exit (Figures 3D and 6C,D). Airflows were 0.5/4.5, 1/4, 1/9, 2/8 (ml/s odor/ml/s continuous), which means that for each airflow, setting air speed decreased with increasing tube diameter. Exhaust speed was 0.4 m/s.

Effect of suction of the exhaust system

We investigated the effect that an exhaust tube had on pulse integrity. We used commercial hose (11-cm outer diameter, 8-cm ID, a thin plastic skin supported by a helix of wire coiled along its length). The exhaust flow rate was modified to produce a range of intake exhaust speeds at 0, 0.4, 1, 1.5, 2, 3, 4, and 5 m/s. Air speeds at the location of the PID were typically about half of the airflow of the exhaust, that is, 0, 0.2, 0.5, 0.75, 1, 1.5, 2, and 2.5 m/s. The lower values were mathematically extrapolated because our anemometer was

not able to record airflows below 0.4 m/s. The main flow and odor-laden airflows were delivered as described earlier, the PID was stationed 20 mm from the exit of the stimulus tube opening, and the exhaust was 35 mm further downwind from the PID (Figures 3E and 7). Airflows were 0.5/4.5, 1/4, 1/9, 2/8 (ml/s odor/ml/s continuous), which at stimulus tube exit corresponds to air speeds of 0.13 m/s (for 0.5/4.5 and 1/4) and 0.26 m/s (for 1/9 and 2/8).

Detection of odor off of centerline

In order to determine the lateral spread of the signal, that is, how close to the centerline of the airflow must one be to get reliable signals, the PID was placed at centerline distances of 10 and 20 mm downstream of the odor tube (Figures 3F and 8). The PID was then run at centerline (0 mm) and moved at 10-mm distances crosswise to the flow until no signal was detected. This experiment was done with exhaust suction of 1.6 m/s, with the exhaust tubing 55 mm from the stimulus tube exit, which means that the suction caused an estimated air movement of 0.8 m/s at the PID. Airflows were 0.5/4.5, 1/4, 1/9, and 2/8 (ml/s odor/ml/s continuous).

Results

Odorant stimuli of 2-heptanone could be measured using a PID. As an example, the original 3.3-Hz data for an airflow of 2 ml/s odor in 8 ml/s mainstream are presented in Figure 2C. With the PID at −12 mm, the response followed the emission of the odor very closely: this translates into the autocorrelation having a sinusoidal pattern of peaks and troughs with time, high peak-to-trough distances and smooth, curved lines with little irregularity (white line in Figure 2D). When the PID was moved 30 mm from the exit of the tube, coherence decreased and the PID response was jagged and nonuniform (thick black line in Figure 2C). The autocorrelation reflects this, with breakdown in the sinusoidal nature of the line and smaller peak-to-trough distance. There was still some 3.3-Hz periodicity even at this distance (thick black line in Figure 2D). In all remaining figures we only show the initial second (three peaks) of the autocorrelation.

Response curves to odor presentations at 2 ml/s odor and 8 ml/s mainstream flows are presented for the various assays in Figure 3. The first column shows diagrammatic views of the variables tested. The second column shows the PID responses for continuous 3-s pulses. The third column shows the PID responses for 10 pulses of 50 ms at 3 Hz. These data are analyzed as an autocorrelation graph in the fourth column. The graphs are shown as separate figures without overlapping traces in the supplementary material on the Internet (see http://neuro.uni-konstanz.de/PID or supplementary material on the Journals website).

A series of physical parameters were investigated individually and are presented in sequence. An overview is given in

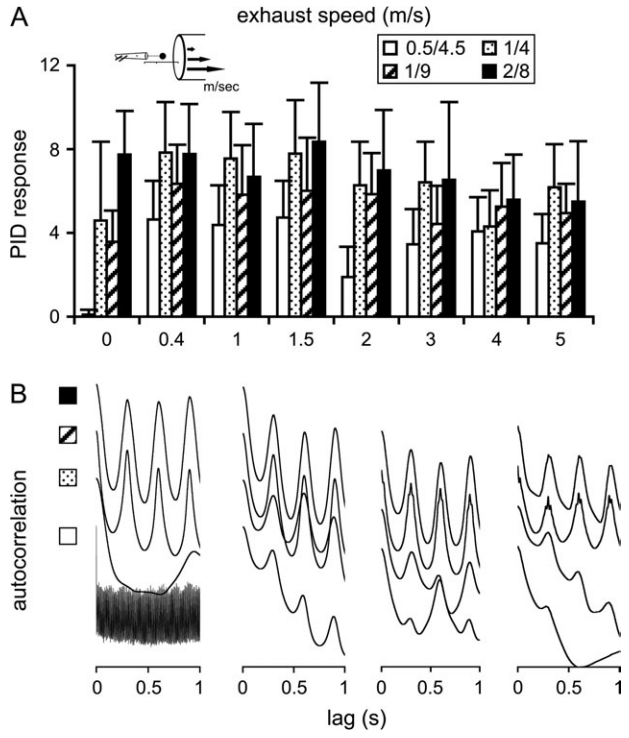

Figure 7 Effect of exhaust air speed (see also Figure 3E). **(A)** PID response at differing exhaust air speeds for continuous 3-s pulses. **(B)** Autocorrelation analysis for selected 3.3-Hz pulses: 0, 1, 3, and 5 m/s.

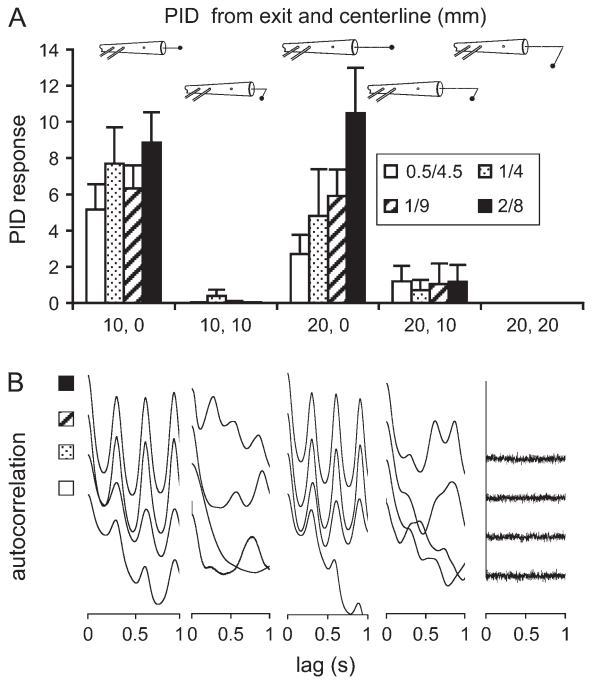

Figure 8 Effect of being off centerline (see also Figure 3F). **(A)** PID response at differing distances off centerline for continuous 3-s pulses at 10 and 20 mm downstream of tube exit. **(B)** Autocorrelation analysis for the 3.3-Hz pulses. Even a small deviation from the central axis leads to a tremendous deterioration of the stimulus.

Figure 3, where each row is one parameter set that is treated in detail in a subsequent Figure (e.g., Figure 3A in Figure 4, Figure 3B in Figure 5, etc.).

Position along airstream

Odor detection at −12 and 0 mm was very consistent in the flatness of the signal during the 3-s pulse, and there was high coherence between the 10 pulses of odor at 3.3 Hz and the PID response (Figures 3A and 4). However, with increasing distance from the tube exit, the measurable odor decreased and the curve became more jagged (Figure 4A, where the bars are mean odor measurements and the error bar is the SD over the 3-s odor delivery as a measure of pulse smoothness). When the PID was placed within the tube or at the exit of the tube, total airflow did not greatly affect the stimulus, and the 3.3-Hz pulses could still be resolved (Figure 4B). However, with increasing distance, the pulsed signal deteriorated greatly (Figures 3Aii and 4B). For example, at 30 mm, stimulus intensity (i.e., bar height in Figure 4A) dropped by more than half even for airflow 2/8. Here, faster airflow led to a more consistent pulsed stimulus. This high flow was the only airflow in which there were remnants of the temporal structure of the pulsed stimulus, as shown by the somewhat sinusoidal trace of the autocorrelation (Figure 4B).

Effect of exit tube length

When 8- and 16-cm extensions were placed on the end of the exit tube with the PID at the terminus (Figure 3Bi), the response of the PID to the 3-s pulse decreased and onset of the response was delayed (Figures 3Bii and 5A). Odor pulses appeared to be "smeared" by a longer tube, and consequently discrete odor pulses lost their individuality and fused, as shown by the lack of structure in the autocorrelation for the 8-cm-long and the 16-cm-long tubes (Figure 5B). Because this effect might result from different air speed across the tube diameter, we investigated whether an increased airflow could at least partially compensate for this effect. Results are shown in Figure 5C: with the 16-cm extension and the 3.3-Hz pulses, low airflow (1/4) produced almost no response, and an intermediate airflow (2/8) showed a recognizable albeit ragged response. A distinct saw tooth pattern with high coherence was restored by using higher airflows (4/6 and 4/16), indicating that increased airflow can help maintain the temporal structure of a stimulus. Investigating how a long odor delivery tube might affect the temporal presentation of different chemicals or of components in an odor mixture was beyond the scope of this study.

Effect of exit tube diameter

Tube diameter greatly affected signal integrity. With the 3-s pulse at 10 mm, the three largest tube diameters provided a jagged PID response curve, whereas the smallest diameter produced the closest approximation to the square pulse (Figure 3Cii). However, there was a delay in the onset of the signal for the smallest tube diameter (Figure 3Cii), which was reproducible when the assay was replicated (data not shown). The 3-s signals at the 10-mm distance were higher magnitude than at 20 mm (Figures 3C,D and 6A,C). Regarding the 50-ms pulses, at 10-mm distance, the two intermediate diameters showed good coherence (Figures 3Civ and 6B). At 20 mm and with the largest diameter tubing, the coherence was poor (Figures 3Div and 6D). For both distances and the smallest tubing, the 50-ms pulses at 3.3 Hz were virtually undetectable with a concomitant dissolution of any coherence (Figures 3C,D and 6B,D). Overall, tube diameter settings followed an optimum curve: both very small diameters and very large diameters led to a deterioration of pulse integrity. With an exit diameter of 4.8 mm, PID intensity did not reflect odor concentration but rather absolute quantity, in that airflow of 0.5/4.5 had the least signal, 2/8 the most, whereas airflows 1/4 and 1/9 had the same and intermediate amount of odor (Figure 6A). However, at 20-mm distance airflow had a greater effect, with faster airflow leading to better pulse integrity. It should be noted that in this experiment, delivered air volume and tube diameter were variables that together affected air speed. At 5 ml/s (as in the airflow 0.5/4.5 and 1/4 settings) and with a tube diameter of 1.3 mm, air speed at tube exit was 3.8 m/s resulting in a 50-ms pulse of 188-mm length and an inter-pulse length at 3.3 Hz of 1076 mm. With a diameter of 9 mm, air speed dropped to 0.079 m/s, and a 50-ms pulse was less than 4-mm long.

Effect of suction of the exhaust system

All experiments reported so far were conducted in a hood with a continuous air speed of 0.4 m/s pulling along the odor delivery axis. We therefore investigated the effect of changing the exhaust air speed (Figures 3E and 7). With the PID stationed 20 mm downwind of the odor exit and the exhaust tube 35 mm downwind of the PID, the speed of the exhaust affected pulse integrity. With no exhaust (speed 0 m/s) and slow stimulus airflow (airflow 0.5/4.5), both the 3-s pulse and the train of short pulses could not be reliably detected.

Best results were obtained with intermediate suction between 0.4 and 1.5 m/s. In this range, PID measurements qualitatively reflected odor concentration (Figure 7A) and the train of 3.3-Hz pulses could clearly be resolved (Figures 3Eiii and 7B). At airflows 1/9 and 2/8, our stimulus had a speed of 0.26 m/s. An exhaust speed of 1 m/s resulted in a measurable airflow at the PID of 0.5 m/s. Therefore, these data suggest that exhaust should be set to withdraw air at a speed that is higher than stimulus speed. However, when suction was further increased, stimulus integrity decreased both in amounts of odor detectable (Figure 7A) and in coherence of the patterned pulses (Figure 7B).

Detection of odor off of centerline

This experiment was done with an exhaust air speed of 1.6 m/s at the opening of the exhaust tube (i.e., 0.8 m/s at the PID).

Responses on centerline for 10 and 20 mm confirmed previous experiments in that signal detection was better at the shorter distance and faster airflows (Figures 3F and 8A,B). When the PID was moved perpendicularly from the centerline, the signal deteriorated quickly for both the 3-s and 50-ms pulses. At 10-mm offset with 10-mm distance from exit and at 20-mm offset with 20-mm distance, there was almost no odor detection (Figures 3F and 8A,B). For the 50-ms pulses, there was only close coherence for the centerline positions (Figures 3F and 8B). We expect this effect to underestimate the situation in physiological experiments because the PID actively aspirated air, while an insect's antenna or a mammalian mucosa in a sniff-restrained animal does not.

Discussion

For any investigation in sensory physiology, good control over the physics of the stimulus is at the base of a quantitative understanding of sensory processing. Just as a perfect control of light wavelength and intensity is necessary for vision research, control of the spatiotemporal presentation of olfactory molecules is necessary for olfactory investigations. In aquatic systems, mixing an odorant with a visual marker, such as a fluorescent substance, allows representation of odor plumes, and thus a quantification of the actual stimulus (Weissburg and Dusenbery, 2002). For airborne odors, no comparable system is available. However, a PID can be used to monitor odor concentration at a particular point with high temporal resolution (Justus *et al.*, 2002a).

Here we demonstrate that a parcel of odorized air translocated through the tubing of an odor delivery device can vary considerably in the final signal profile that passes over an experimental animal's receptor organ. The results imply that in olfactory research, any experimental result with a component of complex temporal patterns in neuronal activity has to be interpreted with great caution. It is important, therefore, to give sufficient thought to the degradation of the airborne signal through the device or in the few centimeters beyond the exit of the odor delivery system. Clearly, the pulse of odorized air does not maintain its consistency from the emitter to the target animal. Depending on the goal of the research, the final odor packet can vary so greatly as to mar the interpretation of the data and the conclusions reached.

We found that the structure of an airborne odorant stimulus changes when it is released from the tube, where the airstream changes from a laterally restrained flow into an unrestrained open space. All parameters we investigated had an effect on the temporal structure of the stimulus: airflow, distance from tube exit, distance from the odor source within the tube, tube diameter, speed of air movement downstream of the delivery system, and lateral distance from tube axis. For some parameters, an optimal setting can be achieved. For example, airflow had an optimal function: too little and too much both affected pulse integrity. Given how interrelated we found the effects of these settings to be, we cannot report values for optimal settings, but suggest that each setup should be calibrated independently. Furthermore, we manipulated but a few parameters of our system, leaving many options open to improve or decrease stimulus integrity. Among others, factors to be taken into account are tubing material, air switching valves, experimental rig, as well as odorant concentration, odor mixture effects, adsorption of odor molecules along the system, and turbulence within the system.

Stimulus integrity deteriorated within 10–30 mm from tube exit. We consider this to be a typical distance used by researchers between exit of the odor delivery apparatus and the experimental animal: a literature meta-analysis (40 papers) showed that the distance between odor delivery and insect antenna was reported in the Materials and Methods in less than half of the papers. Of the remaining papers, 50% gave a distance ≤20 mm and up to 90 mm in the remainder. The most accurate temporal control was achieved within the odor tube itself. In an insect preparation such as those that we commonly deal with, the ideal situation would therefore be to insert the insect's antenna into the odor tube. Even for insects that have antennae of a suitable length, this is not always possible because such a setting would limit accessibility for physiological measurements (e.g., electrodes at the antenna), so that a compromise must often be accepted. In the compromise situation, the best is a medium-diameter odor delivery tube, fast but not too fast odor delivery speed, and slightly faster air suction along the same axis as the odor tube (which means a much larger volume of exhaust air as compared to stimulus air). Also, the distance between odor delivery into the airstream and the experimental setup should be as close as possible: an odor pulse is altered as it travels along a tube, thus losing the sharp onset and offset rates.

One experimental concern that we did not investigate directly is the effect of adsorption of odors onto the inner surfaces of our flow system and their possible reentrainment into the airstream. That the pulsatile nature of the stimulus was well preserved in the "optimal" setup of this system argues that these phenomena had little effect on our findings. However, we caution that other odorant chemicals may be more susceptible to adsorption/reentrainment and that the magnitude of these effects would be contingent on factors such as the duration of odor flow in the system, stimulus concentration, rate of airflow, the materials used (glass, various plastics, etc.), and the physical configuration. In one olfactometer used to study pulsatile signals (Cardé *et al.*, 1984), the off-phase of the delivery system had a backflow, regulated by a flip-flopping airstream. The odor-laden airflow within the apparatus was shunted between the outflow (stimulus on) and exhaust line (stimulus off) by a Coanda wall. This arrangement eliminated odor delivery during the off cycle, including reentrainment of odor molecules adsorbed to the apparatus wall.

Our investigation was inspired by studies in insect olfaction, in which odors are delivered to the antenna of an

immobilized insect. In other situations the constraints will be different. For example, when odors need to be delivered to a rodent that probes an odor port, air turbulence might be less of a concern, given that the animal's snout would be held within the odor port (Uchida and Mainen, 2003; Abraham *et al.*, 2004). However, the result that distance from odor source within the tube strongly affects the resolution of a pulsed stimulus and the steepness of odor onset would also apply to this situation.

Our finding that pulse coherence is affected by several variables implies that some results found in the literature regarding temporal patterns should be interpreted with caution. Without knowing the stimulus integrity of the odor it is not possible to verify whether a physiological recording of great undulation represents the physiological organization of a sensory response or whether it is an accurate reflection of the stimulus available to the receptors. For example, in a study of odor responses in the honeybee antennal lobe, odor responses not only consisted of stereotypical glomeruli being activated, but also were temporally complex (Sachse and Galizia, 2002). At that time, it was thought that a better understanding of the local neuron network in the antennal lobe would hold the key to understanding that complexity. However, according to results of the current study, it is apparent that some of that complexity could have been due to subtle variations in signal intensity. That is, temporal olfactory responses may not necessarily be attributed to the insect's neural circuitry but, instead, may reflect the quality of the odor stimulus, which is subject to the physical parameters measured in this study. It is therefore advisable to use a PID in future experiments to ensure an accurate monitoring of the stimulus' temporal structure. Unfortunately, not all odors can be detected by a PID. An alternative approach would be to use an excised antenna and measuring an electroantennogram (EAG) response to monitor fluctuations in odor intensity (Murlis *et al.*, 2000; Vickers *et al.*, 2001; Stopfer and Laurent, 2002). However, because the sensitivity of EAGs is dependent on what odor is used, this might not always be a suitable solution.

These findings have implications that go beyond experimental design. Odor plumes are highly stochastic in nature (Murlis *et al.*, 1992). The pattern contained in the repeated pulses that we tested was not conserved for any significant distance from the odor source. Therefore, as has also been shown in aquatic systems, odor stimuli are temporally complex and chaotic (Weissburg, 2000). At any single point in time, an animal that smells a particular odor cannot predict the temporal sequence of pulses of that odor in the immediate future. Similarly, in a sender–receiver situation, such as a female moth releasing pheromone plumes to attract a male, the sender has no control over the temporal patterns of odor present in the plume and available to the male. The fast temporal domain is dictated by physical properties of air turbulence and the size of the odor source (Murlis *et al.*, 1992). Indeed, measurements from whole moth antennal preparations suggest that sensory information is already low-pass filtered at the level of the sensory neurons, whereas longer time scales remain unaffected (Justus *et al.*, 2005). The shredding of pheromone plumes by turbulence directly affects the behavioral response of male moths to pheromones (Mafra-Neto and Cardé, 1995). On a longer time scale, however, periodic release of substance might be maintainable, as shown for arctiid moths that protrude their pheromone gland in a rhythmic fashion (Cardé and Roelofs, 1973; Conner *et al.*, 1980).

An absence of information in the fast temporal structure does not mean that there might not be temporal information about a stimulus within the olfactory system of the perceiving animal. In particular, many invertebrates flick their antennae or antennules and mammals sniff: these sampling regimes may impose a temporal structure onto the olfactory input that could be stronger than the chaotic structure of the stimulus. However, these temporal patterns are created by the sniffing animal itself. In a similar manner, usage of temporal structures in olfactory coding in the brain might be feasible if there is no reliable information within the fine-scale temporal structure of the stimulus itself.

The overall conclusion from this study is that olfactory stimulus integrity in an experimental setting is affected by several parameters of the odor delivery device. Stimulus integrity is maximal within the odor delivery tube or as close as possible to the exit of the tube where the odor emanates and centered on the airflow axis. Second, the odor should be introduced as close to the exit as feasible. Third, exhaust airflow should be in the same direction as the odor-laden air flowing over the insect's sensory structures and should slightly exceed odor delivery speed. Finally, no conclusions should be drawn about temporal response properties unless the stimulus itself has been monitored physically with high temporal resolution.

Supplementary material

Supplementary material can be found at http://www.chemse.oxfordjournals.org.

Acknowledgements

We thank Silke Sachse and an anonymous referee for very useful comments. Thanks also to Christine Dittrich for help with the figures.

References

Abraham, N.M., Spors, H., Carleton, A., Margrie, T.W., Kuner, T. and **Schaefer, A.T.** (2004) *Maintaining accuracy at the expense of speed; stimulus similarity defines odor discrimination time in mice.* Neuron, 44, 865–876.

Baker, T.C., Hansson, B.S., Löfstedt, C. and **Löfqvist, J.** (1988) *Adaptation of antennal neurons in moths is associated with cessation of pheromone-mediated upwind flight.* Proc. Natl Acad. Sci. USA, 85, 9826–9830.

Barrozo, R.B. and **Kaissling, K.E.** (2002) *Repetitive stimulation of olfactory receptor cells in female silkmoths* Bombyx mori *L.* J. Insect Physiol., 48, 825–834.

Bau, J., Justus, K.A. and **Cardé, R.T.** (2002) *Antennal resolution of pulsed pheromone plumes in three moth species.* J. Insect Physiol., 48, 433–442.

Cardé, R.T., Dindonis, L.L., Agar, B. and **Foss, J.** (1984) *Apparency of pulsed and continuous pheromone to gypsy moths.* J. Chem. Ecol., 10, 335–348.

Cardé, R.T. and **Roelofs, W.L.** (1973) *Temperature modification of male sex pheromone response and factors affecting female calling in* Holomelina immaculata *(Lepidoptera: Arctiidae).* Can. Entomol., 105, 1505–1512.

Christensen, T.A., Heinbockel, T. and **Hildebrand, J.G.** (1996) *Olfactory information processing in the brain: encoding chemical and temporal features of odors.* J. Neurobiol., 30, 82–91.

Conner, W.E., Eisner, T., Vander Meer, R.K., Guerrero, A., Ghiringelli, D. and **Meinwald, J.** (1980) *Sex attractant of an arctiid moth* (Utetheisa ornatrix)*: a pulsed signal.* Behav. Ecol. Sociobiol., 7, 55–63.

Finger, S. (1994) Origins of Neuroscience. A History of Explorations into Brain Function. Oxford University Press, New York.

Galizia, C.G., Joerges, J., Küttner, A., Faber, T. and **Menzel, R.** (1997) *A semi in-vivo preparation for optical recording of the insect brain.* J. Neurosci. Methods, 76, 61–69.

Heinbockel, T., Christensen, T.A. and **Hildebrand, J.G.** (1999) *Temporal tuning of odor responses in pheromone-responsive projection neurons in the brain of the sphinx moth* Manduca sexta. J. Comp. Neurol., 409, 1–12.

Johnson, B.N., Mainland, J.D. and **Sobel, N.** (2003) *Rapid olfactory processing implicates subcortical control of an olfactomotor system.* J. Neurophysiol., 90, 1084–1094.

Justus, K.A., Cardé, R.T. and **French, A.S.** (2005) *Dynamic properties of antennal responses to pheromone in two moth species.* J. Neurophysiol., 93, 2233–2239.

Justus, K.A., Murlis, J., Jones, C. and **Cardé, R.T.** (2002a) *Measurement of odor-plume structure in a wind tunnel using a photoionization detector and a tracer gas.* Environ. Fluid Mech., 2, 115–142.

Justus, K.A., Schofield, S.W., Murlis, J. and **Cardé, R.T.** (2002b) *Flight behaviour of* Cadra cautella *males in rapidly pulsed pheromone plumes.* Physiol. Entomol., 27, 58–66.

Kauer, J.S. and **Firestein, S.** (1995) *Methods for air-borne and aqueous stimulus delivery in olfactory research.* In Spielman, A.I. and Brand, J.G. (eds), Experimental Cell Biology of Taste and Olfaction. CRC Press, Boca Raton, FL, pp. 91–97.

Mafra-Neto, A. and **Cardé, R.T.** (1995) *Influence of plume structure and pheromone concentration on upwind flight of* Cadra cautella *males.* Physiol. Entomol., 20, 117–133.

Murlis, J., Elkinton, J.S. and **Cardé, R.T.** (1992) *Odor plumes and how insects use them.* Annu. Rev. Entomol., 37, 505–532.

Murlis, J., Willis, M.A. and **Cardé, R.T.** (2000) *Spatial and temporal structures of pheromone plumes in fields and forests.* Physiol. Entomol., 25, 211–222.

Rumbo, E.R. and **Kaissling, K.E.** (1989) *Temporal resolution of odour pulses by three types of pheromone receptor cells in* Antheraea polyphemus. J. Comp. Physiol. A, 165, 281–291.

Sachse, S. and **Galizia, C.G.** (2002) *Role of inhibition for temporal and spatial odor representation in olfactory output neurons: a calcium imaging study.* J. Neurophysiol., 87, 1106–1117.

Slotnick, B. and **Schellinck, H.** (2001) *Behavioral methods in olfactory research with rodents.* In Simon, S.A. and Nicolelis, M.A.L. (eds), Methods in Chemosensory Research. CRC Press, Boca Raton, FL, pp. 21–61.

Stopfer, M. and **Laurent, G.** (2002) *Odor plume features are encoded across ensembles of locust antennal lobe neurons.* Program No. 660.9. 2002 Abstract Viewer/Itinerary Planner. Washington, DC: Society for Neuroscience. Available from http://sfn.scholarone.com/itin2002/ Accessed February 23, 2006.

Uchida, N. and **Mainen, Z.F.** (2003) *Speed and accuracy of olfactory discrimination in the rat.* Nat. Neurosci., 6, 1224–1229.

Vickers, N.J., Christensen, T.A., Baker, T.C. and **Hildebrand, J.G.** (2001) *Odour-plume dynamics influence the brain's olfactory code.* Nature, 410, 466–470.

Weissburg, M.J. (2000) *The fluid dynamical context of chemosensory behavior.* Biol. Bull., 198, 188–202.

Weissburg, M.J. and **Dusenbery, D.B.** (2002) *Behavioral observations and computer simulations of blue crab movement to a chemical source in a controlled turbulent flow.* J. Exp. Biol., 205, 3387–3398.

Willis, M.A. and **Baker, T.C.** (1984) *Effects of intermittent and continuous pheromone stimulation on the flight behavior of the oriental fruit moth,* Grapholita molesta. Physiol. Entomol., 9, 341–358.

Zwaardemaker, H. (1889) *On measurement of the sense of smell in clinical examination.* Lancet, 1, 1300–1302.

Accepted January 31, 2006